J. Mater. Shaping Technol. (1990) 8:149–158

The Double Reverse Olsen and Stretch–Draw Tests for Evaluating Adhesion of Metallic Coatings on Sheet Steel

K.M. Pickett, G.J. Fata, and D.J. Meuleman

Abstract. Two simulative forming tests for assessing the adhesion of metallic coatings on sheet steel, the double reverse Olsen adhesion test and a new test, the stretch–draw adhesion test, are contrasted. The strain states, the nature of the test results, and the responses of various hot dip galvanized and electroplated zinc and zinc alloy coatings are compared. The quantitative mass loss measurements of both tests are shown to have greater relevance than the qualitative visual rating system most commonly used with the double reverse Olsen test. Both tests effectively differentiate good and poor adhesion of alloy coatings. Only small amounts of zinc coatings are lost in both tests. The double reverse Olsen test is easier to perform but represents a sequence of strain states seldom encountered in actual stamping operations.

Introduction

The adhesion of a metallic coating as applied to a steel substrate for corrosion protection is important to both steel and automotive manufacturers. Poor coating adhesion can lead to increased galling tendencies, reduced formability, powder build-up in the dies causing dents and burnished areas, and decreased corrosion resistance. Several methods of determining metallic coating adhesion have been developed. These tests include ball impact stretching, bend testing, shrink flanging (cup drawing), sliding friction or draw bead testing, tensile taping, and die taping. These tests are generally qualitative in nature and, therefore, are of limited value from a research standpoint in defining the major effects to develop new products.

Production automotive stampings are subjected to multiple forming operations. Single mode deformation processes, most commonly used in laboratory evaluations of coated steel products, may not realistically predict material press performance. Therefore, adhesion tests that use multiple deformation stages would better simulate actual material performance. These tests include redrawing and reverse redrawing tests [1, 2], the double reverse Olsen test, [3], and the stretch–draw adhesion test described in this study. Forming factors that influence metallic coating adhesion are plastic strain, strain path, contact pressure, die materials, and associated tribological characteristics. The redrawing and reverse redrawing tests described by Aoki et al. indicate that zinc layer separation does occur and may be affected by the drawing rate in the redrawing test and by previous deformation caused by the first drawing stage in the reverse redrawing test. Although the development of strain causes loss of coating, it has been shown that a change in strain path during forming may heighten loss of metallic coatings [1].

The failure mechanism of a coating can be described as either flaking or powdering, depending upon the type of coating and mode of deformation [2, 4–6]. Flaking refers to a loss of coating by separation from the steel substrate due to the relatively small bonding force at the interface [5]. Powdering refers to a loss of coating by a flaking condition on a small scale. Powdering is not necessarily limited to actual separation at the coating–substrate interface, but can also occur within the coating itself. The fac-

The authors are with the National Steel Corporation, Product Application Center, 12261 Market Street, Livonia, MI 48150, USA.

tors believed to influence the powdering resistance include coating microstructure, composition, and thickness [6]. Flaking and powdering can also be associated with tooling interactions [2, 4–6]. The common characteristics between flaking and powdering mechanisms appear to be linked to the shearing stresses affecting the coating as a result of straining [4, 6].

The double reverse Olsen adhesion test was developed to predict metallic coating adhesion in actual stamping press operations [3]. The test consists of stretching a flat blank in a traditional Olsen test to a fixed dome height, then removing and reversing the sample so that the dome is facing toward the punch. The dome is then pushed through the die opening to a fixed final height. Two different methods are used for analysis. The qualitative method ranks material performance by visual comparison to a photographic standard. The quantitative method is based on total mass loss.

The stretch–draw adhesion test was developed in order to simulate the production forming methods while allowing a change in strain path to occur. The test incorporates a balanced biaxial strain followed by cylindrical cup drawing. It is theorized that the biaxial strain will crack or lessen the integrity of the coating allowing zinc layer removal upon deep drawing. Coating adhesion is quantitatively determined by actual mass loss on the formed sample. The stretch–draw adhesion test is considered severe because of the high level of deformation and the compressive nature of the deep drawing process.

This study compares the stretch–draw and double reverse Olsen adhesion tests. The strain paths, surface areas tested, and results on a variety of metallic coated steels are contrasted. The preferred test is the one which best and most reproducibly predicts actual press performance.

Test Materials

A total of four electrogalvanized and three hot dipped galvannealed materials were used in this study, Table 1. The electrogalvanized materials included zinc (EG), zinc–iron alloy (EGA) and zinc–nickel alloy (Zn–Ni). The hot dipped galvannealed (GA) materials included products which demonstrated good and poor coating adhesion assessed via prior screening tests. All materials were aluminum killed drawing quality products with comparable gages and mechanical properties.

Table 1. Test Materials

Coating Type	I.D.	Coating Type
Electrogalvanized	EG	70G/70G
Electro zinc–iron alloy	EGA-1	50G/50G
Electro zinc–iron alloy	EGA-2	50G/50G
Electro zinc–nickel alloy	Zn–Ni	30G/30G
Hot dipped galvannealed	GA-1	40A/40A
Hot dipped galvannealed	GA-2	40A/40A
Hot dipped galvannealed	GA-3	40A/40A

Experimental Procedure

Double Reverse Olsen Adhesion Test

The double reverse Olsen testing procedure used in this study was modified to include rating by comparison to a visual standard and measurement of coating mass loss using the same sample. The testing was conducted at a strain rate of 2.1 mm/sec with sufficient binder pressure to prevent any drawing of the blank into the die cavity. A thicker lower die was specially fabricated to allow near exact alignment of the initial inverted Olsen dome prior to forming the second dome.

The testing procedure consisted of determining the mass of each 57 mm by 57 mm square sample to the nearest 0.1 mg. The sample was lightly oiled using a mill oil and formed to an Olsen dome height of 8.9 mm. The sample was then inverted and reformed to an Olsen dome height of 6.4 mm. Samples were rated on a scale of 0 to 5 by comparison with visual standards. Mass loss was determined after vapor degreasing and removing loosely adhering coating with filament tape.

Circle grid analysis utilizing 2.54 mm diameter circles [7] and incremental forming of double reverse Olsen test samples were used to define the actual strain path followed during testing. Metallographic cross sections were taken through the center of the double Olsen domes to assess coating integrity.

Stretch–Draw Adhesion

A modified dome test, the Marciniak cup test [8], was used to produce balanced biaxially strained panels from which circular blanks were removed for further testing. In the Marciniak test, materials are mated with a carrier sheet containing a central hole. This combination is completely clamped by a lock bead and deformed to strains of 2, 5, 7, 10, 15, and 20% using a 102 mm diameter flat bottom cylindrical punch. A 70 mm diameter blank was punched from the strained portion of the Marciniak cup. This blank was deburred, vapor degreased, and weighed to the nearest 0.1 mg.

The prestrained blank was lubricated with a polyethylene film–mineral oil combination and deep drawn into a cup using a 32.3 mm diameter flat bottom punch. This combination produced a drawing ratio of 2.16. The cup was vapor degreased and filament tape was applied on both surfaces of the cup to remove the nonadherent coating. After cleaning, the cup was reweighed to the nearest 0.1 mg. The remaining metallic coating then was chemically removed so that the total amount of coating on the original 70 mm blank could be determined. Mass loss was calculated by subtracting the mass of the taped and cleaned cup from the mass of the original blank. The fraction of coating lost was calculated by the ratio of mass loss to the total coating mass.

Metallographic cross sections and scanning electron microscope (SEM) surface views of the top and sides of the drawn cups were examined at each prestrain condition to assess coating integrity and the effect of prestrain on coating adhesion.

Results and Discussion

Double Reverse Olsen Adhesion Test

The double reverse Olsen specification [3] requires visual ratings of 3.5 or less and total coating mass loss of 13 mg or less for material acceptance. Results from this study indicate that the ratings obtained by comparison to a visual standard and by coating mass loss accurately assess coating adherence. This relationship is illustrated in Figure 1. All materials that would be considered acceptable by visual rating fell below 13 mg mass loss, while materials that failed the visual ratings had mass loss in excess of 13 mg. The overlap in mass loss measurements for adjacent visual rating values reflects the subjective nature of visual rating scales. The quantitative measurement

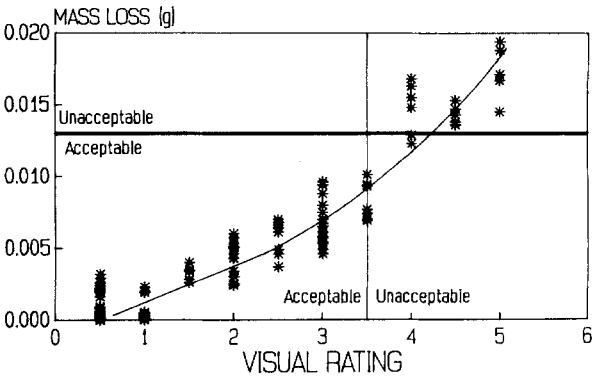

Fig. 1. Double Olsen—mass loss vs. visual rating.

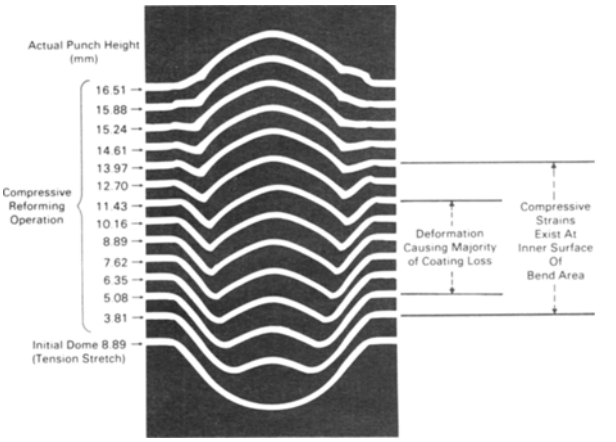

Fig. 2. Incremental forming of double Olsen dome.

of mass loss is a more reliable method of evaluating metallic coating adherence.

Double Reverse Olsen—Strain Path Analysis

The strain path of the double reverse Olsen test was studied by using circle grid analysis with the representative materials and by incremental forming to assess changing strain states. In the double reverse Olsen test the initial Olsen dome is inverted and reverse formed (Fig. 2). This reforming process consists primarily of a compressive bend and straighten operation with bend radii continually decreasing to less that $1T$. The inner dome of the double Olsen button is essentially created by 11.4 mm of punch travel. The remaining 5.0 mm of punch travel pushes the entire inner dome through the original zero point and creates the outer dome. Metallographic examination of dome cross sections revealed that most coating loss occurred in the narrow region where the most severe bend radius was developed.

The strain path for the double reverse Olsen test can be defined as a biaxial stretch (prestrain) followed by a bend and straighten reforming operation. The compressive strain present in this reforming operation is visible in the thickening of the material at the base of the outer Olsen dome.

Stretch–Draw Adhesion Test—Effect of Balanced Biaxial Stretching (Prestraining)

The effect of prestrain on coating loss, both as total mass and as a percentage of the coating present, is shown in Figure 3. The electrodeposited zinc coating was virtually insensitive to prestraining. The electrodeposited zinc–alloy coatings generally exhibited a

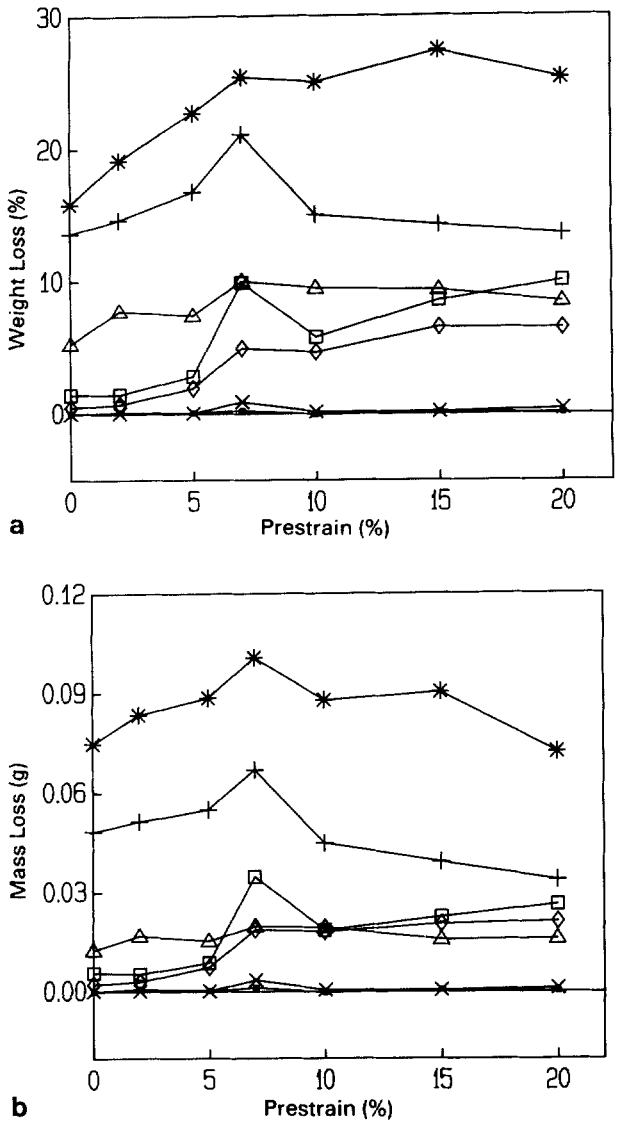

Fig. 3. (a) Effect of prestrain on total percent of coating weight loss; (b) Effect of prestrain on coating mass loss (■ EG, □ GA-1, + GA-2, * GA-3, × EGA-1, ◇ EGA-2, △ Zn–Ni).

low sensitivity to prestraining. The galvannealed coatings exhibited a high sensitivity to prestraining.

Prestraining causes a degradation in the integrity of the metallic coating which depends on the thickness of the metallic coating [1], the coating microstructure, and the particular cracking mechanisms within the coating [1, 4–6]. The amount of degradation is affected primarily by the relative ductility of the coating.

The EG coating produced no cracking through 7% prestrain and only minimal cracking through 20% prestrain (Fig. 4). The coating displayed good ductility, decreasing in total cross-sectional thickness by as much as 25% to 45% (Fig. 5). Other investigations have shown that flaking of EG coatings does not occur until the strain of the substrate approaches its forming limit [5]. Even when highly strained EG coatings cease to deform plastically, substrate deformation is accommodated by the formation of new cracks [4].

The electrodeposited alloy coatings did not display a reduction in coating cross section. All exhibited through-thickness cracking of the coating. Flaking in the coating was not observed (Fig. 6). The typical morphology of the surface cracking pattern is shown in Figure 7. Both Zn–Ni and EGA materials have similarities with EG in relation to flaking mechanisms. Flaking does not occur in the Zn–Ni coatings until the strain in the substrate reaches its forming limit [9]. The EGA materials exhibit some ductility, thus restraining flaking, due to the phase composition ratio [10] and the relative homogeneity of the coating.

The hot dipped GA coatings displayed through-thickness cracking as well as intercoating fragmentation, (Fig. 8). The morphology of the surface cracking pattern was similar for all GA coatings as shown in Figure 9. Other investigations have shown that GA coatings have excellent adherence to the steel substrate in an undeformed state, but the poor ductility of the coating results in cracking of the coating under tensile strains, and the potential for severe powdering of the coating under compressive strains [5]. Distinct layering of zinc iron phases are present in both commercial and laboratory produced galvanneal coatings [11]. Poor coating adhesion can be attributed to the presence of a gamma layer at the steel substrate interface in excess of approximately 5% of the total coating thickness and/or total threshold iron content in the coating in excess of 10% [11, 12]. In this study, the GA sample with the thinner gamma layer had better adhesion than the GA sample with the thicker gamma layer (Fig. 10).

Another effect of prestraining concerns the total amount of coating that is retained on the material being strained. Prior studies have defined a relationship between the original coating mass per unit surface area and coating mass per unit area after prestraining as the effective coating weight [1, 5]. With the increased surface area generated in some deformation processes, the effective coating mass per unit surface area after deformation will be less than the original coating mass per unit surface area. Figure

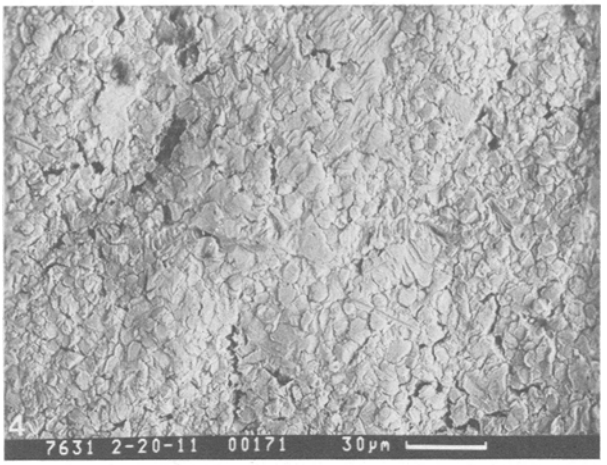

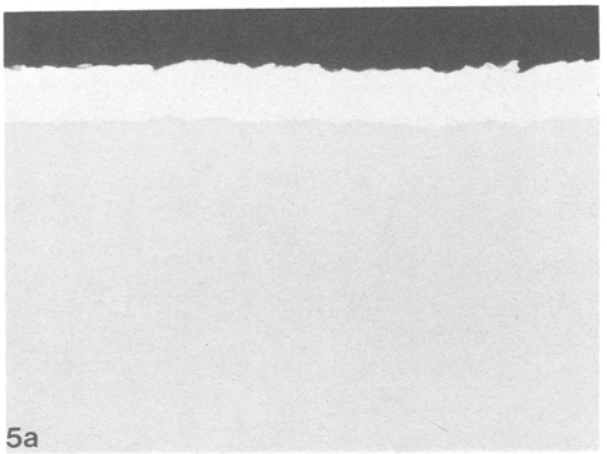

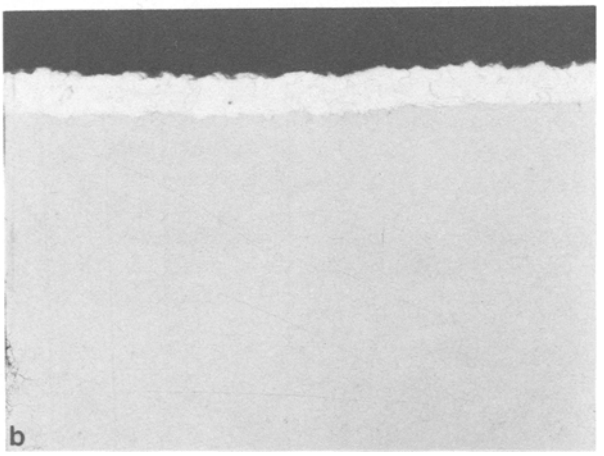

Fig. 4. Surface morphology of electrogalvanized zinc after 20% prestraining detailing cracking pattern (SEM backscattered image, 500×).

Fig. 5. Electrogalvanized zinc detailing a 25% reduction in cross-sectional thickness after 7% prestraining. [½% Nital etch, 1000×.] (a) As received. (b) Prestrained 7%.

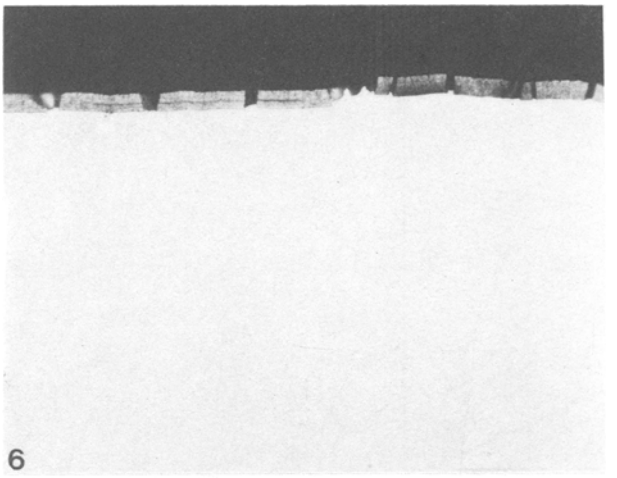

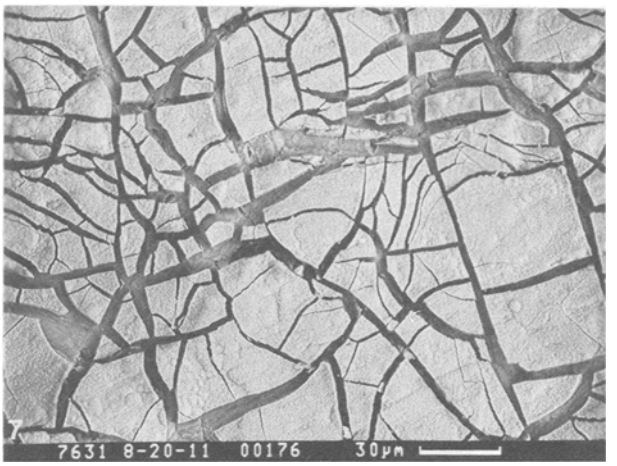

Fig. 6. Typical through-thickness cracking of electrodeposited alloy coating, electrodeposited zinc–nickel alloy prestrained 7% (½% Nital, 1000×).

Fig. 7. Typical surface morphology of electrodeposited zinc alloy coating, electrodeposited zinc–nickel alloy prestrained 20% (SEM backscattered image, 500×).

11 illustrates the linear relationship between the calculated decrease in total coating mass on a 70.0 mm diameter circular blank as a result of prestraining and the actual measured coating mass. This relationship implies good correlation between prestrain and coating mass per unit area reduction, with the exception of the GA-3 material. This material had the thickest gamma layer resulting in the poorest coating adhesion. The actual decrease in coating mass after prestrain was approximately 10% greater than the expected loss from increased surface area, indicating that coating was removed during prestraining. As can be seen in Figure 12, large particles of coating are missing from the surface, reflecting a flaking phe-

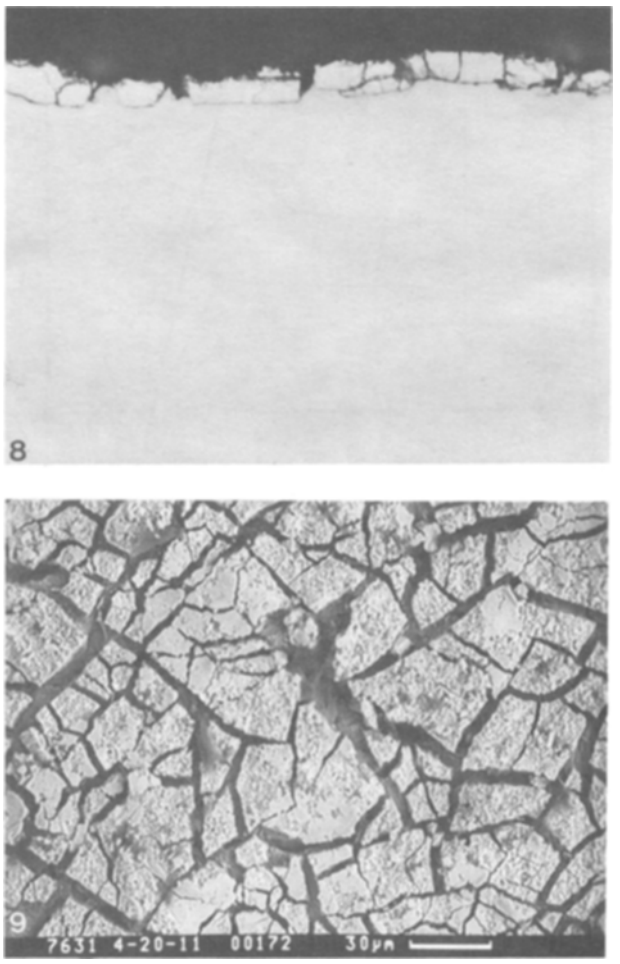

Fig. 8. Typical through-thickness cracking of hot dipped galvannealed materials. GA-2 prestrained 7% ($\frac{1}{2}$% Nital, 1000×).

Fig. 9. Typical surface morphology of hot dipped galvannealed materials. GA-2 prestrained 20% (SEM backscattered image, 500×).

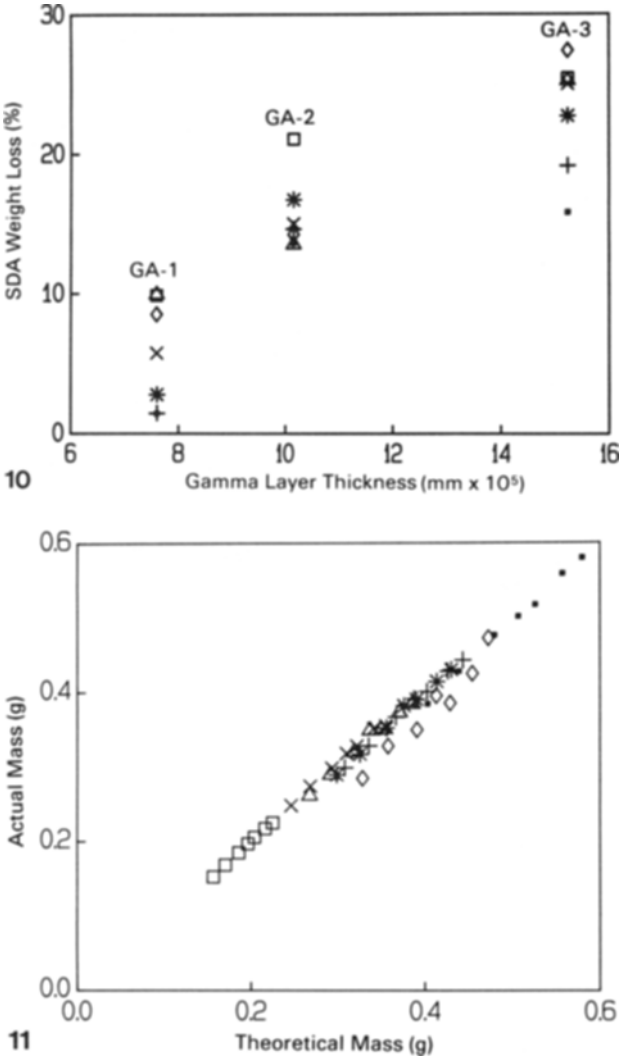

Fig. 10. Effect of alloy layer thickness on total percent of coating weight loss for hot dipped galvannealed material (% Strain: ■ 0, + 2, * 5, □ 7, × 10, ◇ 15, △ 20).

Fig. 11. Comparison of theoretical coating mass (based on unstrained coating mass per unit area and amount of prestrain) and actual measured coating mass on 70 mm diameter circular blanks taken from materials prestrained between 0 and 20% (% Strain: ■ EG, + EGA-1, * EGA-2, □ Zn–Ni, △ GA-1, × GA-2, ◇ GA-3).

nomenon not normally associated with biaxial stretching of galvannealed coatings [4–6].

Stretch–Draw Adhesion—Effect of Deep Drawing

The typical behavior of metal coatings when subjected to deep drawing or shrink flanging operations is well documented [1, 2, 4–6]. The deformation of materials using deep drawing is also accompanied by abrasion along the die face and bending/unbending deformation at the die radius [2]. Adhesion of the coating will depend on the reaction of the coating to this abrasion and the bending/unbending processes as well as the prestrain and compressive strain generated in the drawing process. The different coatings tested were found to react differently.

Stretch–Draw Adhesion—Strain Path Analysis

There is a difference in the amount of coating removed between the inside and outside surfaces of the cup. This difference is more pronounced at higher levels of prestrain. The EG and EGA materials ex-

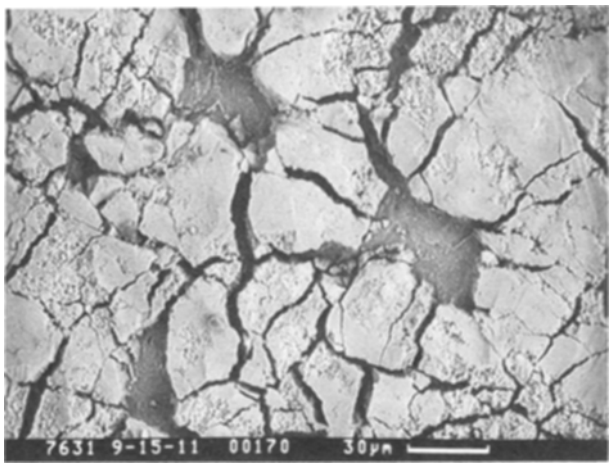

Fig. 12. Hot dipped galvannealed coating detailing typical cracking morphology and apparent flaking condition. GA-3 prestrained 15% (SEM backscattered image, 500×).

perienced a greater coating loss on the outside surface of the cup (Fig. 13) while the Zn–Ni and GA materials had a greater coating loss on the inside surface of the cup (Fig. 14). The actual strain path involved in cup drawing consists of a compressive bend followed by a tension straightening on the outside surface of the cup as it is being drawn through the die opening. Similarly, the inside surface is subjected to a tension bend followed by a compressive straightening. A schematic representation of the tooling used for deep drawing is given in Figure 15. The difference in coating loss between the outside and inside surfaces of the cup may be attributed to any or all of the following variables:

- The ductility of the coating may have an effect. Ductile coatings will deform under both tensile and compressive stresses. Brittle coatings crack in tension and are susceptible to powdering in compression.
- Material in the compression bend on the outside surface of the cup is subjected to a normal force over the die lip. This area would also be subject to any surface/tooling reactions not eliminated by the polyethylene/lubricant combination, Figure 15 (Area A).
- The tension bend on the inside surface of the cup occurs with no normal force. Surface/tooling reactions would be minimal, Figure 15 (Area B).
- Both surfaces are affected by the same strain paths; however, the order of compression and tension are reversed.
- The metal coating interaction with the polyethylene/mineral oil lubricant combination affects each material differently.

It is believed that the major difference arose from the metal coating interaction with the polyethylene/mineral oil lubrication combination. The tension bend without normal force (Area B) causes the polyethylene to stretch over the entire bend. As new cracks are initiated, the polyethylene is stretched even further. As the material is subjected to the subsequent compressive straightening, the polyethylene becomes entrapped between the remaining fractured particles of the coating. Heat generated during the forming of the cups may also contribute by allowing the polyethylene to become more pliable. Noticeable amounts of coating were removed from the inside surface of the Zn–Ni and GA materials when the polyethylene sheet was removed from the cup. The EG and EGA materials did not display this condition.

Comparison of Results

Comparison of results between the double reverse Olsen and stretch–draw adhesion test reveal a consistent trend with respect to mass loss measurements. This trend is shown in Figure 16. All materials passed the double reverse Olsen mass loss requirement of 13 mg except the GA-3 material. Mathematically equating the relative surface area of the double reverse Olsen test dome to the stretch–draw adhesion final cup wall (where the coating loss occurs) yields an equivalent mass loss of 72 mg.

The results obtained by the comparison of double reverse Olsen visual rating to total percentage stretch–draw adhesion weight loss are illustrated in Figure 17. By using the double reverse Olsen mass loss requirement for comparison, these results show that acceptable coating adhesion is represented by losses in coating mass per unit surface area of less than 20%. Specific differences between these two adhesion tests are related to the time required for testing, reliability of results, complexity of test procedures and strain state relative to actual press forming conditions. The speed and simplicity of testing makes the double reverse Olsen test appealing in production and incoming material acceptance situations. However, the accuracy of this test is affected by the variability in operator procedure, equipment limitations, and the subjectivity of visual ratings. The use of mass loss measurement offers greater accuracy, but more time is required to produce results. Also, the strain path of this test holds little relevancy when

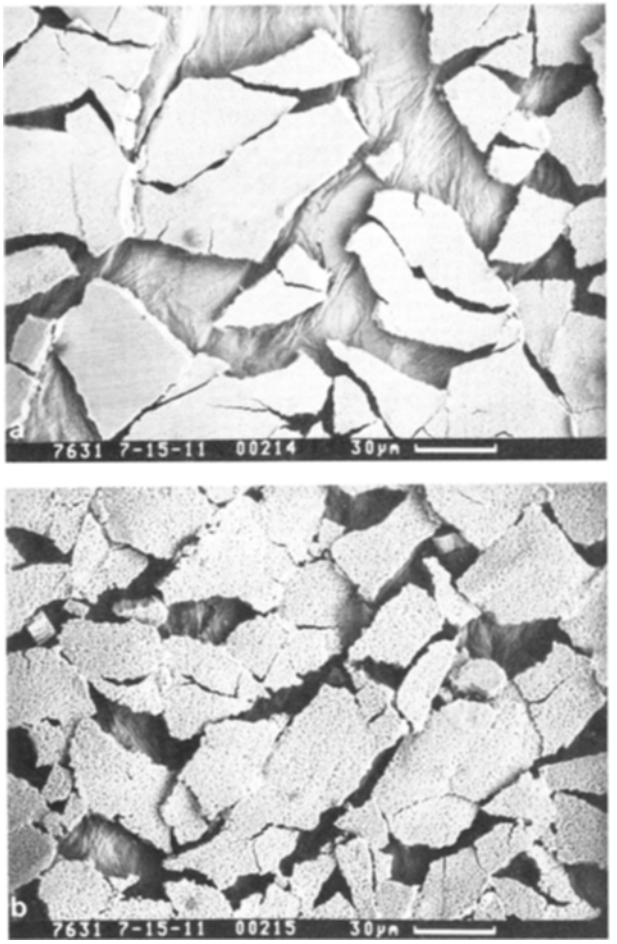

Fig. 13. Typical surface morphology of sides of deep drawn cups for ductile coatings and coatings with limited ductility. [EGA-2 prestrained 15%, SEM backscattered image, 500×.] (a) Outside surface. (b) Inside surface.

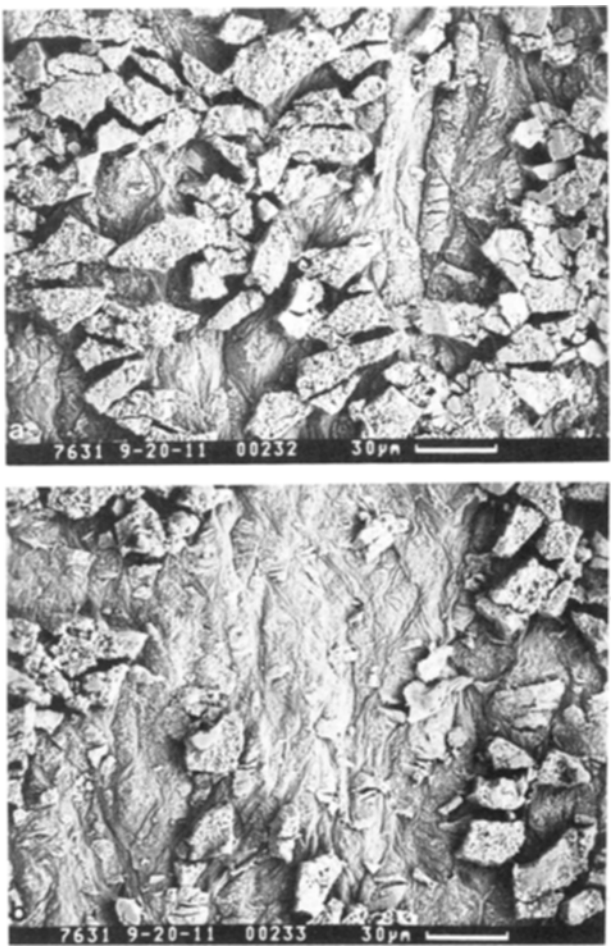

Fig. 14. Typical surface morphology of sides of deep drawn cups for brittle coatings. [GA-3 prestrained 20%, SEM backscattered image, 500×.] (a) Outside surface. (b) Inside surface.

considering actual stamping processes. Few stamping operations involve the drastic reforming over small radii with superimposed compression that occurs in this test.

The stretch–draw adhesion test is also dependent on operator technique and requires more time and sophisticated equipment to produce results. The accuracy of this method is improved primarily as a result of larger sample size, mass loss measurement, and closer simulation of actual press forming conditions. Specifically, the change in strain path would closely simulate a stretch–draw forming operation. A drawing operation with subsequent restriking or stretching of the initial drawn panel would also represent the same strain path characteristics of stretch–draw adhesion, but in reverse order.

Electrodeposited coatings, such as EG, Zn–Ni and EGA, typically display good metallic coating adhesion. Even with the severe deformation involved, the double reverse Olsen and stretch–draw adhesion tests may not adequately differentiate these materials because of the small variation in results. Both tests do clearly delineate differences among hot dipped galvannealed materials. Other coating adhesion testing methods may be more suitable for electrodeposited materials.

Conclusions

Comparison of the two metallic coating adhesion tests have yielded the following conclusions;

1. The quantitative measurement of mass loss is a reproducible method of evaluating metallic coating adherence in both double reverse Olsen and

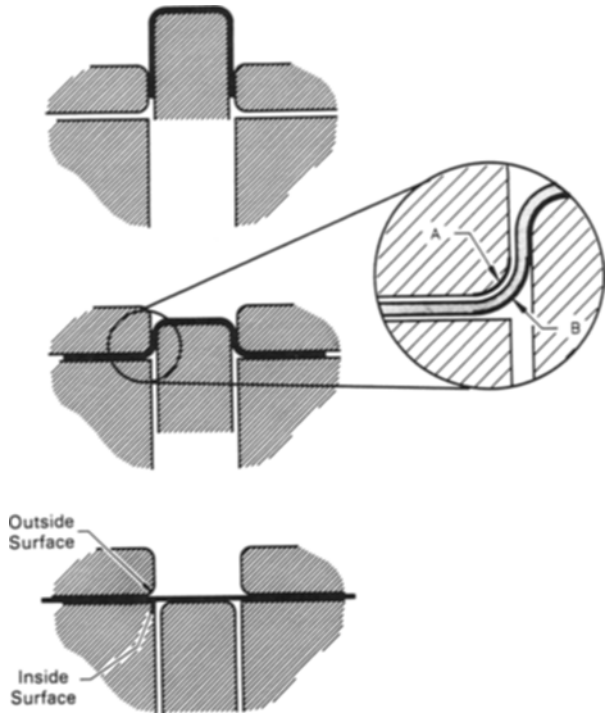

Fig. 15. Schematic depiction of tooling used for deep drawing.

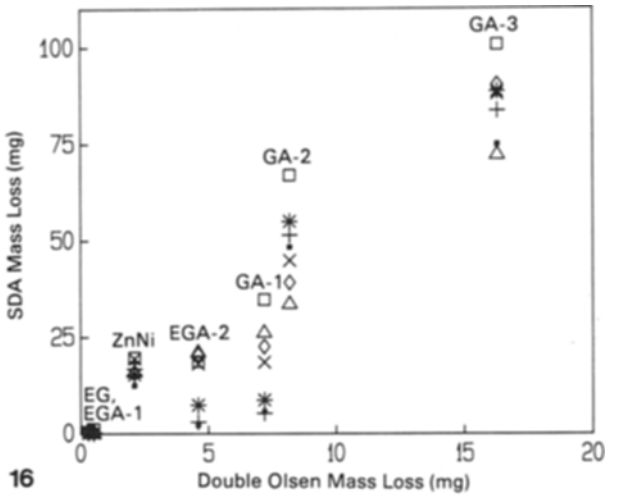

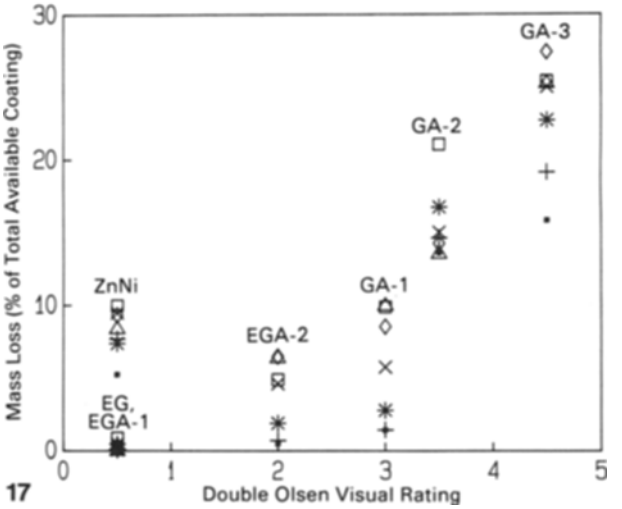

Fig. 16. Correlation of mass loss results between stretch–draw and double Olsen adhesion test (% Strain: ■ 0, + 2, * 5, □ 7, × 10, ◇ 15, △ 20).

Fig. 17. Correlation of stretch–draw total percentage of coating lost and double Olsen visual rating (% Strain: ■ 0, + 2, * 5, □ 7, × 10, ◇ 15, △ 20).

stretch–draw adhesion testing. Results between the two show good correlation.

2. The double reverse Olsen and stretch–draw adhesion tests are most suited to evaluate metallic coating adhesion of GA materials. Little differentiation between electrodeposited coatings was noted by these two tests.
3. As a simulative test to compare coating material performance in actual strain paths involved in press forming, the stretch–draw adhesion test would be considered more appropriate than the double reverse Olsen test.

Acknowledgments. The authors wish to thank National Steel Corporation for the opportunity to publish this work. Special thanks are also extended to Marion Moore for the SEM analysis and Suzanne Ross for the typing of this manuscript.

References

1. I. Aoki, T. Horita, and T. Herai, "Formability and Application of Galvanized Sheet Steels," Technological Impact of Surfaces, ADDRG Conference, 1981, pp. 165–176.
2. M. Shiokawa, H. Takizawa, S. Ujihara, and Y. Hayashi, "A New Method For Evaluating the Powdering Phenomenon of Precoated Sheet Metals," Proc. of the 13th Biennial Congress of the IDDRG, Melbourne, Australia, 1984, pp. 305–316.
3. Chrysler Specification MS-8056, Zinc Iron Alloy Coated Steel For Outer Body Panels.
4. S. Makimattila and A. Ranta-Eskola, "Behavior of Galvanized Coatings During Forming," Proc. of the 13th Biennial Congress of the IDDRG, Melbourne, Australia, 1984, pp. 293–304.
5. C. Sudoo, Y. Hayashi, and M. Nishihara, "Behavior of Coated Film in Press Forming of Surface Treated Steel," Mém. étud. *Sci. Rev. Métall.*, Vol. 77, No. 3, 1980, pp. 353–362.
6. M. Ejima, Y. Tokunaga, and T. Honda, "Analysis of

Formability and Some Problems in Stamping of Coated Steel Sheets," Proc. of the 13th Biennial Congress of the IDDRG, Melbourne, Australia, 1984, pp. 317–328.
7. S. Dinda, K. James, S. Keeler, and P. Stine, *How to Use Circle Grid Analysis For Die Tryout*, American Society for Metals, Metals Park, Ohio, 1981.
8. Z. Marciniak, K. Kuczynski, and T. Pokara, *Int. Journal of Mech. Sci.*, Vol. 15, 1973, pp. 789.
9. A. Shibuya, T. Kurimoto, M. Nishihara, S. Wakano, and T. Kurashige, "Properties of Ni–Zn Alloy Plated Steel, Technological Impact of Surfaces," ASM, 1981, pp. 333–347.
10. T. Hara, T. Adaniya, M. Sagiyama, T. Honma, A. Tonouchi, T. Watanabe, and M. Ohmura, "The Phase Composition and Workability of Electrodeposited FeZn Alloy," Trans. ISIJ, Vol. 23, No. 11, 1983, pp. 954–958.
11. G. Smith, D. Gomersall, and D. Hreso, "Control of Adhesion in Galvannealed Products," Proc. of the 31st Mechanical Working and Steel Processing Conference, Chicago, 1989, pp. 3–8.
12. Y. Tokunaga, M. Yamada, M. Nakayama, N. Henmi, and H. Matsubara, "Some Factors Influential To Adhesion Properties of Galvannealed Steel Sheet," 105th ISIJ meeting, April 1983, Lecture #S343.